

Chapter Five: A *piggyBac* Transposon Screen *In vivo* for Genetic Cooperative Partners of *Trp53* in Gliomagenesis

Abstract

TP53 is amongst the most commonly mutated genes in low grade and high-grade gliomas, suggesting it occurs early in the evolution of these tumors. Large-scale sequencing studies of gliomas from patients have provided a wealth of information on the genetic and epigenetic landscapes of these tumors. However, there is a need for functional studies to identify the precise roles of the many genes that are altered in these tumors, including which and how genes may cooperate with *TP53* alterations in driving tumorigenesis. Here, we have generated cohorts of mice with a conditional *Trp53* mutation and *piggyBac* transposition expressed under the control of *nestin-cre* in the central nervous system. Preliminary data showed high-grade gliomas were generated in this context, albeit with a long latency. In order to increase the incidence and reduce the time for tumor formation we are generating similar mice with additional loss of *Pten*. Given the complexity of the breeding strategies with the extensive time necessarily required to achieve these, this study is ongoing at the time of PhD submission. I describe the results thus far and discuss future experiments in this Chapter.

Introduction and Aims

TP53 is activated in response to cellular stresses, and it binds to DNA to activate transcriptional programmes which allow for control of the cell cycle and have the potential to activate cell death. This function is important for tumor suppression, and *TP53* was one of the earliest cancer genes to be described, particularly in the context of patients with germline mutations in *TP53*. These Li-Fraumeni syndrome patients are prone to many cancers including those of the breast, lung, brain and oesophagus [237-240]. Given the critical role of p53 protein in sensing DNA damage, it is not surprising that *TP53* itself or its pathway is mutated in the vast majority of cancers, including gliomas. This includes somatic mutations in cancers as diverse as melanomas and colorectal cancer [241, 242]. Analysis of TCGA data on GBMs and LGGs demonstrated *TP53* is commonly genetically altered in these tumors: 33.1% of GBMs and 51.6% of LGGs have an alteration in this gene. Missense mutations of *TP53* are common - all GBM *TP53* mutations were found in the DNA-binding domain (with the exception of one mutation which was in the tetramerisation motif), suggesting these are functional mutations [27, 28], Fig 5.1 and 5.2. Collectively, these observations suggest there is clonal selection for loss-of-function alterations of *TP53* in GBM.

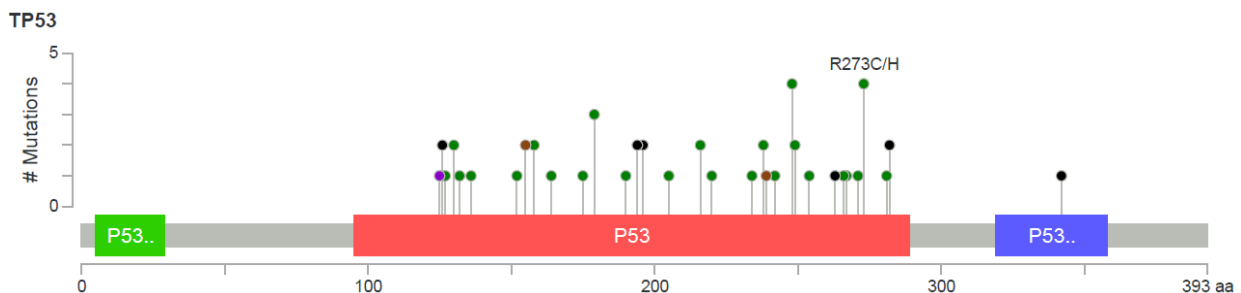


Figure 5.1. This plot demonstrates the number of mutations present in GBMs and where they are located along the amino acid sequence of the p53 protein; each point represents a mutation type and how frequent it is. All mutations are protein coding regions, in particular in the DNA-binding domains of *TP53*, likely abrogating its function as a transcription factor. Green box = *TP53* transactivation domain; red box = DNA binding domain; blue box = *TP53* tetramerisation motif. This plot was generated using CBioportal software, see Materials and Methods.

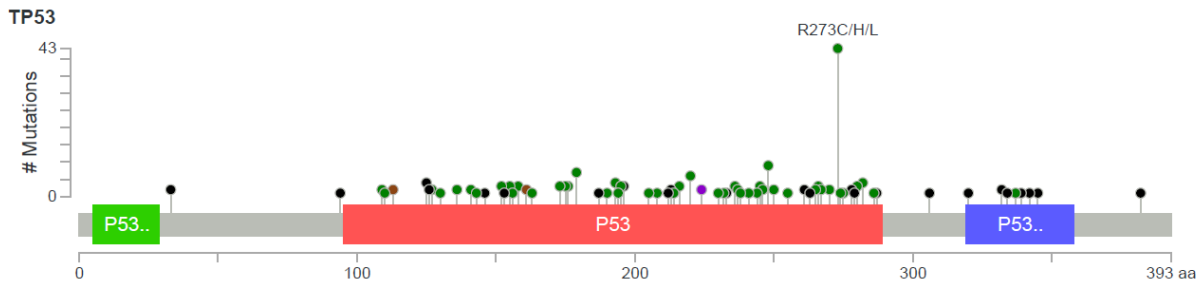


Figure 5.2. Mutations in *TP53* in human LGGs, TCGA dataset. The somatic mutation rate is 51.6%, with 152 missense mutations, 35 truncating, 2 in-frame, and 1 other type of mutation. See previously for descriptions of the protein domain annotations.

The classical view of the role of p53 is that following cellular stress signals such as DNA damage and cellular hyperproliferative signals, MDM2 and MDM4 (negative regulators of p53) are displaced from p53, allowing it to become activated and increase transcription of genes responsible for cell cycle arrest and apoptosis [243, 244]. P53-induced senescence also adds to its tumor suppressive role, for example mice with *Pten*^{-/-} do not develop prostate tumors as quickly as *Pten*^{-/-} *Trp53*^{-/-} mice because p53 induces cellular senescence in the former [245].

Although loss of p53 function itself has tumor promoting effects, there is also evidence that mutant p53 protein has additional gain-of-function oncogene-like properties, for instance disruption of wild-type p53-independent apoptosis [246]. A strong example of this is that genetically-engineered mice which express mutant *Trp53* (*Trp53*^{R172H}) develop a broader spectrum of tumors compared with mice that are heterozygous or null for the wild-type *Trp53* allele: they develop a higher incidence of carcinomas and sarcomas, and have a greater propensity for metastasis and genomic instability, although this type of mutation has been proposed to be a dominant-negative mutation [43, 247, 248]. Oncogenic mutations of *TP53* have been detected in human cancers [249]. Moreover, such oncogenic mutations of *TP53* are also highly expressed [250]. Mutant p53 is thought to have oncogenic properties due to various mechanisms, such as loss of ability to regulate topoisomerase I which normally regulates DNA folding. The G2-M checkpoint is faulty in *TP53*^{R248W} cells, whereas it is normal in *TP53*^{-/-} cells,

further suggesting oncogenic functions of mutant *TP53*. One mechanism proposed to account for these features of p53 mutants is that they interact with the Mre11 nuclease, inhibiting binding of the Mre11-Rad50-NBS1 complex to DNA double strand breaks. This leads to defective Ataxia-telangiectasia mutated (ATM) activation, thus overcoming an important DNA damage response mechanism and promoting carcinogenesis [251]. Over 80% of *TP53* mutations occur in its DNA-binding domain, implying that its role as a transcription factor are critical for its function in tumor suppression [252].

More recently, other roles have been proposed for p53 in addition to its canonical functions. In particular, it is believed that p53 may inhibit invasion and metastasis, enhances communication in the tumor microenvironment, blocks stem cell self-renewal, and inhibits reprogramming of differentiated cells into stem cells [253].

TP53 is one of the most commonly mutated genes in gliomas, found in 20-30% of these tumors. Earlier studies suggested *TP53* is mutated mainly in low-grade gliomas, but more recent work has identified this as a common abnormality in glioblastomas (primary and secondary) too, present in 25-35% of cases [94]. Moreover, *TP53* mutations have been found to occur with *PTEN* loss / mutations in some human GBMs, although mutations in these genes tend to be mutually exclusive in low-grade gliomas, suggesting the combination of mutations in these genes may drive malignant progression [27, 28].

An important study modelling GBMs in mice used GFAP-cre to drive conditional loss of *Trp53* allele in combination with homozygous *Pten* loss; in this model, the cre is expressed throughout the central nervous system, including neural stem cells and mature neurons and astrocytes. Given our success in generating gliomas with *EGFRvIII* expression under nestin-cre control, we decided to use the same approach here by crossing the *Trp53^{R172H}* allele with nestin-cre. This gives strong expression of the conditional allele in the central nervous system (and eye). A study that also expressed a *Trp53* mutant allele under control of nestin-cre employed the *Sleeping Beauty* transposon as a forward genetic screening approach to identify genetic drivers of glioma, however the tumors generated were from *in vitro* rather than *in vivo* transformation of neural stem cells [66]. This study was discussed in the previous Chapter of this Thesis.

***TP53* Mutations in Medulloblastomas**

TP53 mutations are also present in medulloblastomas, albeit at a lower frequency than gliomas [254, 255]. Medulloblastoma (MB) mainly occurs in infants and children, representing the commonest paediatric malignant brain tumor and accounting for 20% of all childhood brain cancers. MB typically occurs in the posterior fossa and has a propensity for metastasis through the cerebrospinal fluid to other sites within the CNS (including brain and spinal cord). It is a high-grade tumor with a typically high proliferative rate. The five-year survival rate with treatment (usually a combination of surgical resection, chemotherapy and cranio-spinal irradiation) is approximately 60%. However, the long-term consequences of treatment are significant, and include neuro-cognitive deficits and neuroendocrine dysfunction [256].

Molecular analyses have demonstrated that there are four major subtypes of this cancer: Wnt-driven tumors (with upregulation of canonical Wnt signalling), Sonic hedgehog (SHh) driven tumors, grade 3 and grade 4 medulloblastomas. This consensus was derived from a multitude of studies, one of the most important being an international study in 2006 demonstrating that MBs can be divided into subgroups according to their transcriptomic profiles, and these subgroups showed intra-group similarities in chromosomal aberrations, mutational profiles, tumor histology and prognosis [257, 258]. The best prognosis, with a 5-year overall survival rate of over 90%, is conferred by the Wnt subtype, whereas the poorest prognosis is conferred by the Group 3 tumors which have a 5-year survival rate of only 40-60%. Group 4 and SHH MBs have an intermediate survival rate of 75%.

The driver genes in each MB subgroup (as determined by significant recurrent mutations and / or copy number aberrations) appear distinct, and are reported as follows [259, 260]:

- Wnt subtype – *CTNNB1* (91%), *DDX3X* (50%), *SMARCA4* (26%), *TP53* (14%), and *KMT2D* (12%).
- SHH subtype – *PTCH1* (28%), *TP53* (14%), *KMT2D* (13%), *DDX3X* (12%), *MYCN* amplification (8%), *BCOR* (8%), *LDB1* (7%), *TCF4* (6%), and *GLI2* amplification (5%).

- Group 3 subtype – *MYC* amplification (17%), *PVT1* amplification (12%), *SMARCA4* (11%), *OTX2* amplification (8%), *CTNDEP1* (5%), *LRP1B* (5%), and *KMT2D* (4%).
- Group 4 subtype – *KDM6A* (13%), *SNCAIP* gain (10%), *MYCN* amplification (6%), *KMT2C* (5%), *CDK6* amplification (5%), and *ZMYM3* (4%).

TP53 mutations can occur in any of these subtypes, but in SHH-altered MBs in particular *TP53* mutations may portend a poorer prognosis and treatment failure [261]. A previous *Sleeping Beauty* transposon screen in mice which employed a *Trp53* mutation as a predisposition allele demonstrated that *Sleeping Beauty* transposition both accelerated and increased the incidence of tumor formation. This was also true in a screen in mice which had a *Ptch1* mutation as a predisposition for a *Sleeping Beauty* transposon screen [56]. Importantly, this study demonstrated that there was a different pattern of common insertion sites (putative genetic drivers) in the metastases compared with the primary medulloblastoma. The authors validated some of these findings through whole-exome sequencing of paired primary medulloblastomas and metastases from a small number of human patients.

Aims

In this set of experiments, we set out to determine the driver genes cooperative with *Trp53* that are necessary for glioma tumor formation and progression *in vivo*. In order to do this, we generated mice containing *Trp53*^{R172H} [43] and *piggyBac* transposition alleles (in addition to control cohorts of mice), and collected the resulting tumors from the brain and spine for histopathological analysis and analysis of the transposon insertion sites. We anticipated that the resulting tumors would comprise both gliomas and medulloblastomas, given *TP53* is mutated in both types of tumor in humans and that *cre* is expressed in the cerebrum and cerebellum under the nestin-promoter. Given the long times needed for tumor formation in this genetic context, the study is ongoing at the time of PhD thesis submission; the main results thus far will be discussed.

Results:**Clinical Phenotypes of Mice**

Three cohorts of transgenic mice were generated for this study, as described in Materials and Methods – *Trp53^{R172H}/+* ; *ATP1S2/+* ; *TSPB/+* ; *nes-cre/+* (*Trp53^{R172H}-PB* mice), *Trp53^{R172H}/+*; *ATP1S2/+*; *nes-cre/+* (*Trp53^{R172H}-only* mice), and *ATP1S2/+* ; *TSPB/+* ; *nes-cre/+* (*PB-only* mice). The sizes of the cohorts are stated in the Methods. Several mice carrying *Trp53^{R172H}* and *nes-cre* alleles developed abdominal (determined to be hepatosplenomegaly) and lymph node masses, requiring culling (see Tables 5.1 and 5.2). The pathological diagnoses for these individual lesions were not characterised for this study, but are due to loss of one copy of the wild-type *Trp53* allele in tissues leading to oncogenesis, for example lymphomas and sarcomas as previously described [43]. In these cases nevertheless, the brains and spinal cords were still processed for histological assessment of these organs. Some mice carrying *Trp53^{R172H}* and *nes-cre* alleles (particularly in the *Trp53^{R172H}* ; *PB* cohort, but also one mouse in the *Trp53^{R172H}-only* cohort) however did indeed develop neurological signs, in particular seizures, paralysis of one or more limbs, and macrocephaly. The age at which mice started developing these signs was from 36 weeks onwards. All mice, their clinical signs and histology are outlines in Tables 5.1 and 5.2.

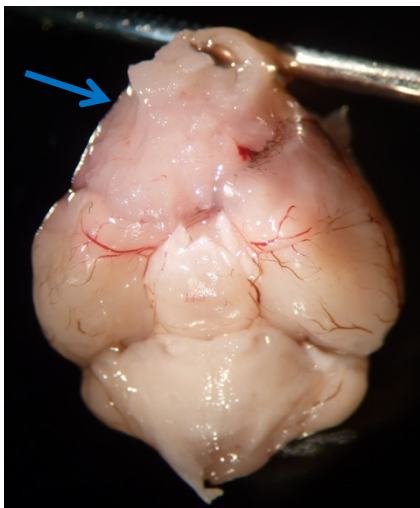


Figure 5.3. Gross inspection of the forebrain of this mouse showed a large tumor, confirmed to be a glioblastoma by histopathological analysis.



Fig 5.4. Low power image of glioblastoma at base of brain in a *Trp53*^{R172H} – PB mouse. The dark stained area in the lower half of the image represents the tumor. Scale bar represents 1mm.

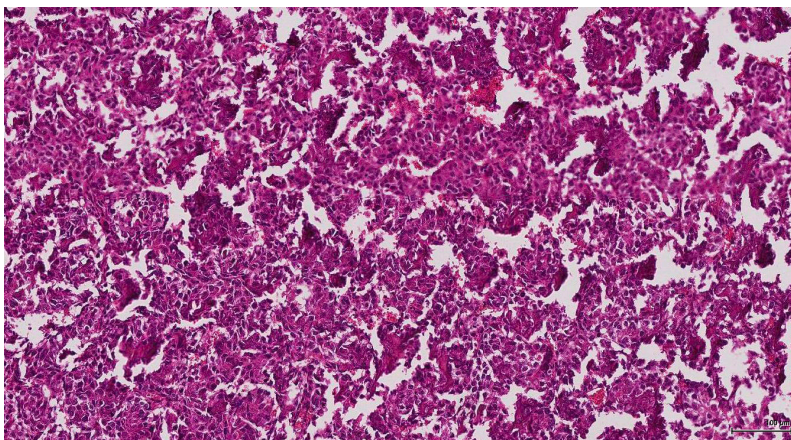


Fig 5.5. Higher magnification image of the glioblastoma from Figure 20. This H&E stained section shows a high cellular density, typical of a high-grade glioma. Scale bar represents 100 μ m.

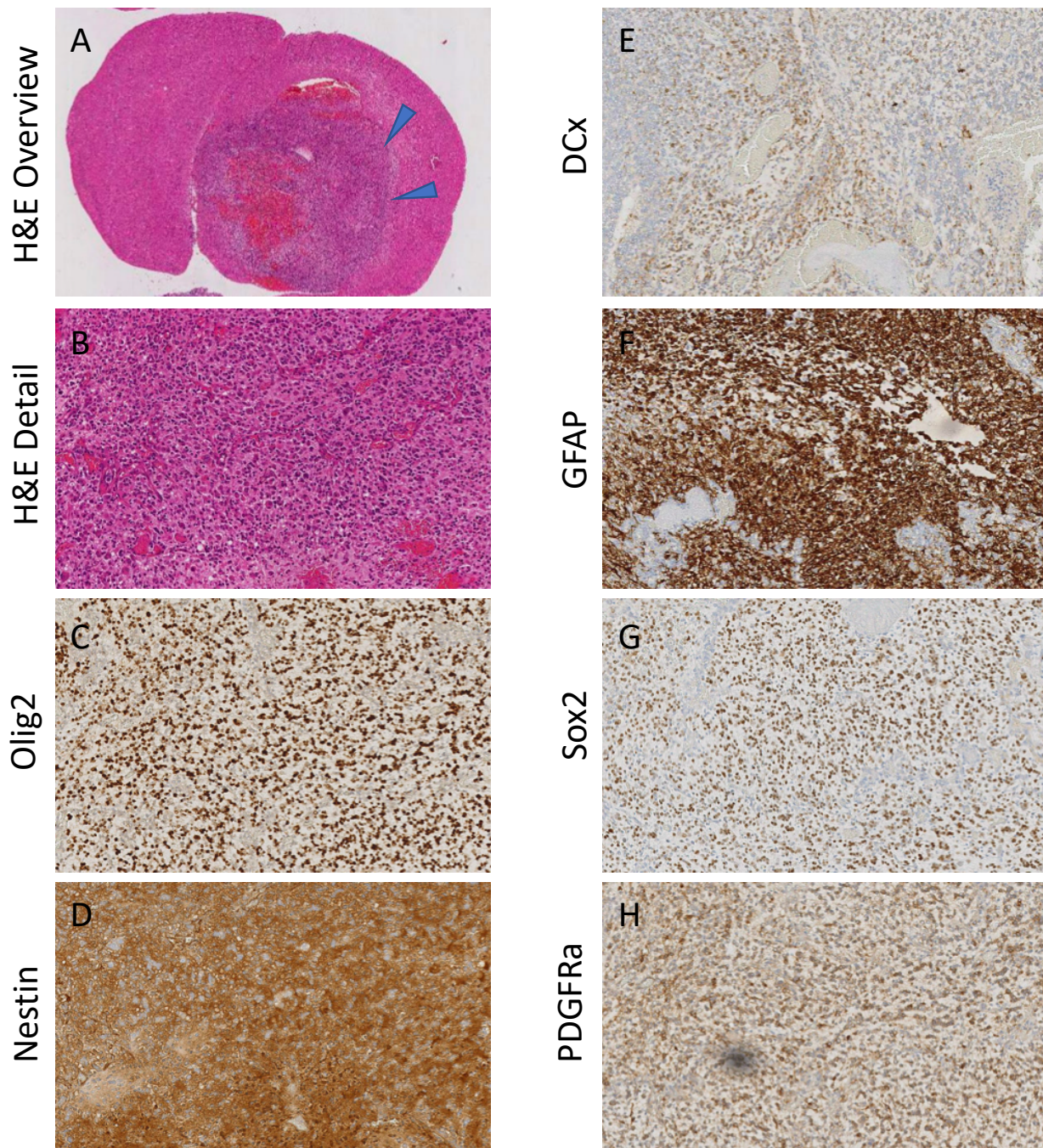
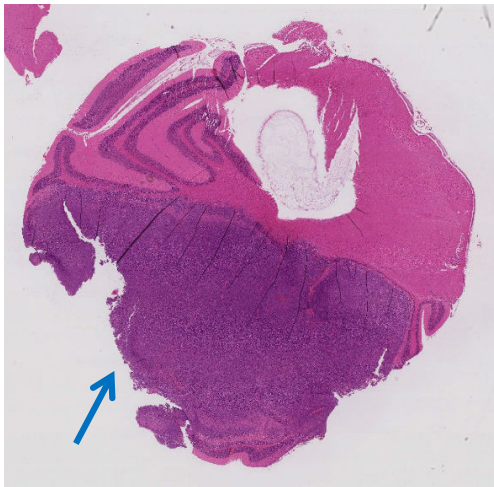


Fig 5.6. Typical example of a glioblastoma from a $Trp53^{R172H}$ -PB with immunohistochemical staining for glioma markers. H&E stains are shown in (a) and (b), Olig2 in (c), nestin in (d), double-cortin in (e), GFAP in (f), Sox2 in (g) and PDGFRa in (h). Scale bar represents 1mm and 100 μ m. See text for further details, and see Materials and Methods for histological criteria for glioma grading. All histopathology in this Chapter and this Thesis was reviewed by Consultant Neuropathologist, Professor Sebastian Brandner.



Medulloblastoma

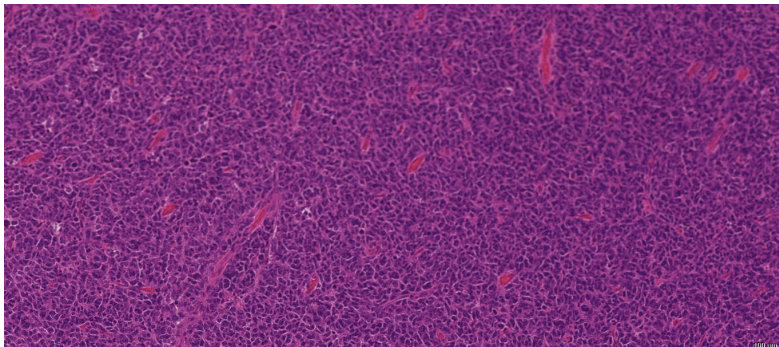


Fig 5.7. Medulloblastoma observed in the cerebellum of a 24.5 week old *Trp53*^{R172H} – PB mouse. Higher power view is seen in the lower panel. This H&E section shows a highly cellular tumor that is poorly differentiated, and the cells contain little cytoplasm; new small blood vessels can be observed in the tumor. Scale bar represents 1.5mm for the upper panel and 100 μ m for the lower panel.

INPF	Age	Signs	Histology (SB Comments)	Spine Pathology
30.1f	24.5	Moribund	Medulloblastoma	No tumor
18.1A	35.4	Swollen abdomen, hunched	No tumor	No tumor
24.1a	32.5	Sunken abdomen, hunched	No obvious pathology	No tumor
19.1c	40.2	Swollen abdomen, hunched. Necropsy - enlarged liver and spleen.	No tumor	No tumor
19.3f	36.2	Hunched, rapid breathing	No tumor	No tumor
26.1f	39	Swollen abdomen; hunched	Grade 4, giant tumor (glioma)	No tumor
18.1c	46.2	Reduced and uncoordinated movement, piloerection	No tumor	No tumor
18.3g	42.4	Paralysed	No tumor	Malignant soft tissue tumor in spine, not related to spinal cord
18.2d	50.2	Hunched, rapid breathing, piloerection, inactive	No tumor	Epidermoid tumor in spinal cord
18.2a	51.6	Culled for urogenital mass	No tumor	No tumor
29.1b	50	Macrocephaly, hunched, piloerection	Expansive, demarcated high grade glioma, haemorrhage (grade IV)	No tumor
19.2b	54.3	Immobile, piloerection	No tumor	No tumor
30.2f	47.6	Moribund, macrocephaly	Large expansive glioblastoma in forebrain (grade IV)	No tumor
29.3b	44.4	Hyperventilation	Isolated tumor islands at the base of brain, pituitary gland? (grade 1/2)	No tumor
25.1e	52.8	Abdominal mass	No tumor	No tumor
25.1g	52.8	Paralysed	No tumor	Astrocytoma, malignant solid tumor
30.1d	51.7	Abnormal behaviour and posture	No tumor	No tumor
14.1c	63.2	Mass under skin	No tumor	Bone tumor invading spinal cord
18.1e	58.2	Abdominal mass, hunched	Intraparenchymal tumor nest, multifocal (grade IV glioma)	No tumor
19.3a	55.3	Hunched, piloerection	No tumor	No tumor
26.2g	65.8	Paralysis	Small island of malignant primitive tumor, frontal basal	Osteoid tumor in thoracic spine

Table 5.1. Table of culled experimental mice, showing clinical details and pathology from the brain and spine. These mice are all heterozygous for *Trp53^{R172H}*, nestin-cre, ATP1-S2 and TSPB (*Trp53^{R172H}* – PB cohort). INPF is the prefix for this mouse colony. SB comments reflects comments from our neuropathologist, Professor Sebastian Brandner.

Thus far in this study, there were 5 gliomas (including one astrocytoma in the spinal cord), one epidermoid tumor, one bone tumor, a medulloblastoma, and a possible pituitary tumor, as confirmed on histopathological analysis of H&E stained sections by a Consultant Neuropathologist, Fig 5.3, 5.4 and 5.5. The youngest age for a mouse in this cohort with a glioma was 39 weeks, and therefore there is a relatively long latency for onset of these tumors in this genetic context. The mouse with a medulloblastoma was only 24.5 weeks old at death.

To confirm the histological diagnosis of GBM in the relevant samples from *Trp53^{R172H}*; PB mice, we performed immunohistochemical staining on 3 tumors for a panel of protein markers that are relevant to human gliomas, Fig 5.6. The results were as follows:

- Olig2 – positive cytoplasmic staining in all tumor cells.
- PDGF α – positive cytoplasmic / membrane (usually diffuse pattern) staining in regions of the tumors.
- Sox2 – positive nuclear staining in all tumor cells (moderately to strongly positive).
- Double-cortin – weakly positive cytoplasmic staining in most areas of the tumors.
- GFAP – cytoplasmic / cell processes are strongly positive in the majority of the tumor.
- Nestin – positive cytoplasmic / cell processes staining, with some tumor-associated vessels also positive.

This staining pattern supports the histological diagnosis of these being glial tumors (see Materials and Methods for the grading system we used).

INPF	Age	Signs	Histology (SB Comments)	Spine Pathology
11.2A	25.5	Uncoordinated (but likely general illness)	Multiple small SVZ clusters; subarachnoid spread of small round cells, possibly lymphoma	Negative
27.1c	35.8	Swollen toe.	Negative	Subdural tumor growth
11.3a	48.4	Leg mass (likely lymph node abnormality)	No tumor	No tumor
20.1f	54.2	Reduced movement	No tumor	No tumor
14.2d	57.6	Uncoordinated movements, hunched, lethargic	Primitive, well demarcated neuroectodermal tumor (grade IV)	No tumor
14.1d	44.7	Mass under skin	Normal	Subdural tumor growth
14.2h	45.2	Swollen abdomen	No tumor	No tumor
14.1e	75	Paralysis	No tumor	Osteoid tumor in lumbar spine
14.2a	49	Seizures	No tumor	No tumor

Table 5.2. Table of culled control mice, providing clinical details and pathology of the brain and spine.

All of these mice are heterozygotes for: *Trp53*^{R172H}; nestin-cre. They lack transposase and thus *piggyBac* transposon is not mobilised.

Relatively few control mice with *Trp53*^{R172H}-only (with no transposition) required culling at the time of submission of this thesis, despite the median age of this cohort being 48 weeks. As can be observed from the table, one mouse brain showed evidence of proliferation of SVZ and subarachnoid space round cells, although these were not tumors. Two mice had small subdural glioma-like growths. One mouse developed a high-grade brain tumor, which was a primitive neuroectodermal tumor (PNET) on histological analysis; this unusual type of tumor was not present in the *Trp53*^{R172H} - PB mice. In no case was a glioblastoma observed, unlike in the *Trp53*^{R172H}-PB cohort. However, meaningful Kaplan-Meier curves of survival times of mice from both cohorts cannot yet be drawn given the majority of mice are still alive. Therefore, additional observation time is required for the remaining mice to determine whether these observations will be reflected across all mice in this study.

Discussion

In this study, we generated cohorts of *Trp53*^{R172H} mice with and without transposition in order to determine the cooperative driver events that support *Trp53* mutations in gliomagenesis *in vivo*. *Trp53* mutant mice with transposition developed tumors with relatively long latency and low incidence (only 8 confirmed intrinsic CNS tumors after aging mice for one year). This observation strongly argues for the need for additional genetic drivers on a *Trp53* mutant background in order to produce brain and spinal tumors. In the *Trp53*^{R172H} – PB cohort of mice, there were 5 high-grade gliomas confirmed after the mice were aged for one year; in comparison, no high-grade gliomas were seen in the *Trp53*^{R172H} – only cohort, with the exception of one primitive neuroectodermal tumor that was considered to be high-grade although this type of tumor is a distinct entity compared with glioblastoma [262]. Although it remains to be seen whether these observations will be seen in the remaining mice of this study, these findings suggest that *piggyBac* transposition, through altering the appropriate cancer genes, is enabling progression of *Trp53* mutant cells towards a glioblastoma phenotype. It will be interesting to determine if there are significant differences in the pathological spectrum of CNS tumors generated in *Trp53*^{R172H} – PB mice compared with *Trp53*^{R172H} – only mice, and if so to determine the set of genes responsible for pushing *Trp53* mutant cells into a GBM phenotype through mapping of the transposon common integration sites. Moreover, it remains to be seen whether this model with transposition leads to a substantial proportion of medulloblastomas (so far, one has been generated), as this will enable comparison of *Trp53*-cooperative driver genes in gliomas with medulloblastomas.

The idea that certain transposon integrations will favour different tumor types is established, in line with the notion of context-dependent cancer genes. For example, the *piggyBac* screen for pancreatic cancer performed by Rad and colleagues helped elucidate the genetic basis of distinct subtypes of pancreatic cancer. They found that hepatoid pancreatic cancers (a rare subtype) in their mice were enriched with *Fidgetin* (*Fig* – a member of the AAA-ATPase superfamily) *piggyBac* integrations, suggesting this gene may help drive this subtype of pancreatic cancer, although further functional proof is awaited.

In order to ensure a sufficiently large number of tumors is generated to have reliable transposon integration sites, we have also started generating mice with *Trp53*^{R172H} and *Pten* loss in combination with transposition (all with cre driven by the nestin promoter). We anticipate these mice will produce gliomas with a higher frequency than *Trp53*^{R172H} and transposition alone, given that *Trp53* and *Pten* have previously been shown to synergise in driving glioma formation in mice [94]. Having mice with this combination of alleles will also help elucidate the influence of different initiating mutations on subsequent genetic evolution of tumors, particularly in comparison with an *EGFRvIII* initiating mutation for which we have data as discussed in previous Chapters.

Although the genetic events that cooperate with *TP53* and *PTEN* loss to drive gliomagenesis are poorly understood, recent work has pointed towards the *QKI* ('quaking') gene as having an important role in this as a putative tumor suppressor. Deletion of *Qki* in mice accelerated glioma formation in a *Trp53* and *Pten* null background, and it was suggested that this was due to enrichment of receptors needed for maintenance of cell self-renewal and therefore stemness, an important aspect of tumorigenesis [263]. Interestingly, *Qki* was a common integration site for *piggyBac* in our *EGFR*-PB screen for gliomas, with a disruptive integration pattern, suggesting deletion of this gene contributes to gliomagenesis in an *EGFRvIII*-driven background as well. It remains to be determined which cooperative partners are specific to having a *Trp53* / *Pten* initiating mutation compared with *EGFR*, and which partners are common across all mutational backgrounds. We hope further work from sequencing tumors generated in this study will help provide the answers to these questions.

Study Limitations

The main limitation of this study is the long times for tumor generation, partly associated with the complex breeding strategies involving multiple breeding steps but also because the latency itself for tumor formation in the experimental mice is rather long. As such further work is required to complete this study, in particular the histopathological analysis needs to be extended to all samples, and there needs to be sequencing to map the *piggyBac* integration sites in the tumors available.

Another limitation is that many mice required culling because they developed tumors outside of the central nervous system. This is because of the known effects of the *Trp53^{R172H}* allele, in that all cells in the mouse will only have one functional copy of *Trp53* (and cells in which recombination occurs because of *nestin-cre* will also express the mutant allele). As a result, there is a known predisposition in these mice to many cancers, particularly lymphomas and sarcomas [43]. Therefore, this precluded a substantial fraction of mice developing the intended brain tumors in our model. A possible way of circumventing this problem and potentially increasing the proportion of intrinsic brain tumors would be to use a conditional *Trp53* knockout allele, in which all somatic cells carry both copies of the functional *Trp53* except cells in which recombination takes place (which will carry only one functional copy). This approach may therefore reduce the fraction of mice developing tumors outside of the nervous system when used with the *nestin-cre* driver.

To establish the cells in which recombination of the *Trp53^{R172H}* allele has occurred in our model, a further important step would be to perform immunohistochemical staining for the mutant protein, using an appropriate antibody that recognises mutant forms of the protein but not wild-type. This experiment is necessary to confirm that gliomas (and medulloblastomas) generated in the model used here are indeed, at least partially, driven by this mutant allele.

Conclusions

Given that most of the mice remain under observation at the time of submission of this Thesis, with only a fraction of mice having been sacrificed and histologically assessed thus far, strong conclusions cannot yet be drawn. However, with further experiments as described above that are needed to comprehensively complete this study, we anticipate this work will be complementary to our work *EGFRvIII*-induced gliomas in helping elucidate the genetic evolution of these tumors.